Am J Cancer Res 2025;15(7):2932-2948
www.ajcr.us /ISSN:2156-6976/ajcr0163908

Original Article

USP13 mediates resistance to Ibrutinib in diffuse large B-cell lymphoma via augmenting FHL1 stabilization

Yun Tao[1,2*], Haibing Yin[1*], Rong Shen[1], Song He[1], Xiaobing Miao[1]

[1]Department of Pathology, Affiliated Tumor Hospital of Nantong University, No. 30, Tongyang North Road, Nantong 226361, Jiangsu, China; [2]Department of Clinical Laboratory, Affiliated Hospital of Nantong University, No. 20, Xisi Road, Nantong 226006, Jiangsu, China. [*]Equal contributors.

Received February 13, 2025; Accepted June 18, 2025; Epub July 15, 2025; Published July 30, 2025

Abstract: Diffuse large B-cell lymphoma (DLBCL) is the most common type of lymphoid malignancy in the world which is mainly divided to ABC type and GCB type. Ibrutinib benefits patients with ABC subtype DLBCL by inhibiting Bruton's tyrosine kinase (BTK), but there are still a lot of patients who are resistant to Ibrutinib. In this study, we found that post-translational modification played a regulatory role in mediating Ibrutinib resistance in DLBCL. The expression of USP13 was significantly higher in Ibrutinib-resistant U2932 cells compared with Ibrutinib-sensitive WSU-DLCL2 cells, and its expression was further increased both in WSU-DLCL2 and U2932 after exposure to Ibrutinib. USP13 overexpression significantly promoted cell growth and decreased Ibrutinib sensitivity in DLBCL while knockdown of USP13 significantly increased Ibrutinib-induced apoptosis and improved the sensitivity to Ibrutinib. Further studies showed that USP13 interacted with FHL1 and stabilized the expression of FHL1 via deubiquitination, thereby mediating the phosphorylation of ERK1/2, resulting in the decrease expression of Bax and the increase expression of Bcl-xL, thus mediating Ibrutinib resistance in DLBCL. The results of immunohistochemical staining of tumor tissue also indicated that the expression level of USP13 was negatively related to the prognosis of DLBCL patients. These new findings provided an experimental basis for overcoming Ibrutinib resistance in DLBCL and showed that USP13 is a potential therapeutic target and prognostic marker in DLBCL.

Keywords: Apoptosis, DLBCL, FHL1, Ibrutinib, USP13

Introduction

Diffuse large B-cell lymphoma (DLBCL) is the most common lymphoid malignancy in adults [1]. DLBCL can be divided into two main subgroups: germinal center B-cell-like (GCB) and activated B-cell-like (ABC) [2]. Rituximab, cyclophosphamide, doxorubicin, vincristine, and prednisone (R-CHOP) is the standard first-line treatment for DLBCL. However, 40% of these patients fail to achieve a complete remission or suffer a relapse [3]. Due to the genetic and biological differences between ABC and GCB DLBCL, patients with ABC DLBCL show less favorable clinical outcomes. The ABC DLBCL is characterized by chronic B-cell receptor (BCR) signaling and activation of nuclear factor κB (NF-κB) pathway via a cascade of kinases, such as spleen tyrosine kinase (SYK), Bruton's tyrosine kinase (BTK) [4]. Ibrutinib, a potent and highly selective inhibitor of BTK, is currently approved for the treatment of chronic lymphocytic leukemia, mantle cell lymphoma, Waldenstrom's macroglobulinemia, and marginal zone lymphoma. It has also been found to kill the ABC DLBCL lines by reducing NF-κB pathway activity. Despite the remarkable success of Ibrutinib in the clinic, drug resistance is a major ongoing challenge [5, 6].

Post-translational modifications such as phosphorylation, ubiquitination, methylation and acetylation are crucial in modulating drug resistance in tumor by regulating oncogene activation, cell cycle regulation, tumor cell metabolism, tumor microenvironment, and cellular immune checkpoint [7]. Ubiquitination and deubiquitination are important post-translational modifications involved in numerous biological functions, such as cell growth, proliferation, apoptosis, DNA damage response. Ubiquitination is a process through which ubiquitin

https://doi.org/10.62347/IMFU7145

chains are attached to substrate proteins for protein degradation. Deubiquitination is the removal of ubiquitin molecules from targeted substrates and is mediated by the deubiquitinating enzymes (DUBs). DUBs are categorized into two major classes, cysteine proteases and metalloproteases [8, 9]. Ubiquitin specific protease 13 (USP13), also known as isopeptidase T-3, is a deubiquitinase member of the cysteine-dependent protease superfamily that cleaves ubiquitin off protein substrates to reverse ubiquitin-mediated protein degradation [10-12]. The structure of USP13 contains a USP domain and a ZnF ubiquitin binding domain. The USP domain contains two UBA domains. USP13 is involved in many cellular processes, such as cell cycle regulation, endoplasmic reticulum related degradation and autophagy. USP13 is also reported to play an important role in inflammation and stress response. Studies have shown that USP13 plays different roles in different tumors. High expression of USP13 in breast cancer is associated with a better prognosis, while in gastric and ovarian cancer it predicts a poor prognosis [7, 13, 14]. USP13 plays a pivotal role in cancer development by affecting NF-κB, AKT/MAPK, TLR4/MYD88/NF-κB signaling pathway, regulating the stability of PTEN, MCL1, MITF, MITF-M and other proteins, regulating the repair of DNA damage, and glucose metabolism [15, 16]. However, the role of USP13 in DLBCL remains unclear.

FHL1 (four and a half LIM domain protein 1), also known as SLIM1, is a cytoskeletal protein that is highly expressed in skeletal and cardiac muscle and mediates protein interactions within the cytoplasm. The LIM domain of FHL1 plays an important role in mediating the interaction between FHL1 with other proteins. FHL1 is involved in various cellular physiological functions, such as cytoskeleton remodeling, cell growth and transcriptional regulation [17]. Moreover, FHL1 has been shown to play an important role in regulating tumor progression. FHL1 may regulate tumor growth by regulating cell cycle and the activation of TGF-β signaling pathway. Overexpression of FHL1 in gliomas is associated with enhanced tumor invasion and migration [18]. However, several findings indicate that FHL1 functions as a tumor suppressor. FHL1 expression was lower in lung adenocarcinoma tissues compared with the normal lung tissues, and high expression of FHL1 was significantly correlated with a better prognosis [19]. FHL1 has been reported to mediate the resistance of tumor cells to radiotherapy by inhibiting CDC25C activity [20]. Zhou et al. [21] reported that FHL1 could promote paclitaxel resistance in hepatic carcinoma cells via regulating caspase-3 activation. However, the role of FHL1 in DLBCL have not yet been identified. In this study, the biological function of USP13 and FHL1 in DLBCL was examined.

Materials and methods

Cell culture, transient plasmid transfection and lentivirus infection

DLBCL cell lines WSU-DLCL2 and U2932 were obtained from Cobioer Biosciences Company (Nanjing, China). WSU-DLCL2 cells were routinely maintained in DMEM medium (GIBCO, Grand Island, NY, USA) supplemented with 10% fetal bovine serum (FBS, GIBCO). U2932 cells were maintained in RPMI 1640 medium (GIBCO) supplemented with 10% FBS. WSU-DLCL2 was exposed to Ibrutinib at a concentration of 13 μM, and U2932 was exposed to Ibrutinib at a concentration of 19 μM. The exposure time for both was 24 hours. HEK293T cells were obtained from Cobioer Biosciences Company, and were incubated in DMEM supplemented with 10% FBS. Flag-tagged USP13, His-tagged FHL1, and Myc-tagged ubiquitin (Myc-Ub) plasmids were obtained from GeneChem Co., Ltd. (Shanghai, China). Transient transfection of plasmids was performed using Lipofectamine 2000 (Invitrogen, Shanghai, China) following the manufacture's protocol. Lentiviral USP13 overexpression vector (USP-13^{OE}), lentiviral USP13 shRNA (shUSP13) and lentiviral FHL1 shRNA (shFHL1) were purchased from the Genechem. USP13 targeting sequences were: AGATAAAGAAGTTCACTTT (shUSP13#1), GGTGAAATCTGAACTCATT (shUSP13#2), and CAGTATCTAAATATGCCAA (shUSP13#3). FHL1 targeting sequence was: TGGTGGCCTATGAAGGACAAT. Lentiviral control-shRNA (shCtrl) sequence was: TTCTCCGAACGTGTCACGT. Lentivirus infection was performed according to the manufacturer's instructions (GeneChem). To establish stable cell lines, lentivirus-infected cells were selected with 2 μg/mL of puromycin (GeneChem).

Western blot

Total protein was collected and equal amounts of total protein were run on SDS-polyacrylamide gel electrophoresis (SDS-PAGE) and transferred to polyvinylidene fluoride (PVDF) membranes (Roche, Basel, Switzerland). The membranes were then blocked with 5% skim milk for 1 h, and incubated with primary antibodies overnight at 4°C. Then the membranes were washed with phosphate-buffered saline (PBS) containing 0.05% Tween 20 (PBS-T) and incubated with the secondary antibody for 1 h. After washed with PBS-T, the membranes were visualized using the enhanced chemiluminescence (ECL) reagents (NCM Biotech, Suzhou, China) and ChemiDoc Touch Imaging System (Bio-rad, Hercules, CA, USA). Antibodies and dilutions were as follows: anti-USP13 polyclonal antibody (1:2000 dilution, Proteintech Group, Wuhan, China), anti-USP13 monoclonal antibody (1:2000 dilution, Invitrogen), anti-FHL1 antibody (1:2000 dilution, Proteintech Group), anti-Flag-M2 antibody (1:1000 dilution, Sigma-Aldrich, St Louis, MO, USA), anti-His antibody (1:5000 dilution, Proteintech Group), anti-Myc antibody (1:2000 dilution, Proteintech Group), anti-Bax antibody (1:1000 dilution, Cell Signaling Technology, Beverly, MA, USA), anti-Bcl-xL antibody (1:1000 dilution, Cell Signaling Technology), anti-ERK1/2 (p44/42 MAPK) antibody (1:1000 dilution, Cell Signaling Technology), anti-phospho-ERK1/2 (p44/42 MAPK) (Thr202/Tyr204) antibody (1:1000 dilution, Cell Signaling Technology), anti-Rabbit IgG isotype control (1:1000 dilution, Cell Signaling Technology), anti-GAPDH antibody (1:5000 dilution, Proteintech Group), Peroxidase AffiniPure Goat Anti-Rabbit IgG (H + L) (1:10000 dilution, Jackson ImmunoResearch Laboratories, West Grove, PA, USA), Peroxidase AffiniPure Goat Anti-Mouse IgG (H + L) (1:10000 dilution, Jackson ImmunoResearch Laboratories).

Immunoprecipitation

For immunoprecipitation (IP), cells were washed with PBS and lysed using IP lysis buffer (NCM Biotech) with protease and phosphatase inhibitor cocktail (NCM Biotech). The cell lysates were centrifuged, and then immunoprecipitated at 4°C overnight using the indicated primary antibodies followed by incubation with Protein A/G beads (Roche) for 1 h. The immunocomplexes were washed twice with IP lysis buffer before being resolved by SDS-PAGE and immunoblotted with indicated antibodies.

Apoptosis detection assay

For cell apoptosis analysis, cells were stained with an APC Annexin V and 7-Amino-actinomycin (7-AAD) (Biolegend, San Diego, CA, USA) according to the manufacturer's instructions. In brief, the cells were washed twice with cold BioLegend's cell staining buffer, and then resuspended in 100 μL of Annexin V binding buffer. Cells were then placed into 5 mL test tubes. Next, 5 μL of 7-AAD and 5 μL of APC Annexin V were added to the tubes and incubated for 15 minutes at room temperature in the dark. Samples were diluted with 400 μL of Annexin V binding buffer and immediately subjected to flow cytometry.

Quantitative real time RT-PCR (RT-qPCR) assay

Total RNA from the WSU-DLCL2 and U2932 cells was extracted by using the RNAprep Pure Cell/Bacteria kit (Tiangen Biotech, Beijing, China) according to the manufacturer's instruction. The isolated RNA was further converted into first strand cDNA with RevertAid First Strand cDNA Synthesis Kit (Thermo Fischer Scientific, Waltham, MA, USA). *RT-qPCR assay* was performed by using SuperReal PreMix Plus (SYBR Green) (Tiangen Biotech) on an Applied Biosystems 7500 real-time PCR detection system. The primer sequences are as follows: *USP13* Forward: 5'-TCTCCTACGACTCTCCCAATTC-3'; *USP13* Reverse: 5'-CAGACGCCCCTCTTACCTTCT-3'; *GAPDH* Forward: 5'-TGACTTCAACAGCGACACCCA-3'; *GAPDH* Reverse: 5'-CACCCTGTTGCTGTAGCCAAA-3'.

Cell counting kit-8 (CCK-8) assay

Cells were seeded on the 96-well plates (Thermo Fischer Scientific) at a density of 1×10^4 cells/well in a volume of 100 μL. CCK8 labelling reagent (10 μL; Dojindo, Kumamoto, Japan) was added to each well and incubated at 37°C for 1 h. Absorbance of the cells was measured at 450 nm using a microplate reader (Molecular Devices, Sunnyvale, CA, USA).

Patients and specimens

A total of 181 cases of DLBCL, diagnosed between January 2012, and December 2018 at the Affiliated Tumor Hospital of Nantong

University, were included in this study. Slides of all cases were reviewed according to the 5th edition of the World Health Organization (WHO) diagnostic criteria. This study was approved by the Ethics Committee of the Affiliated Tumor Hospital of Nantong University.

Immunohistochemistry and assessment of immunohistochemistry

Immunohistochemistry was carried out as described previously [22]. Briefly, sections were deparaffinized in xylene and rehydrated through descending percentages of ethanol to water. Antigen retrieval, elimination of the endogenous peroxidase activity, and blocking were carried out according to standard protocols. The sections were incubated with primary antibodies at 4°C overnight. Primary antibodies used include: 1:300 diluted USP13 (Proteintech Group), and 1:100 diluted FHL1 (Abcam, Cambridge, MA, USA). Following the incubation, the sections were washed with PBS 3 times, and then incubated with HRP-conjugated secondary antibody (Proteintech Group, PK10006) for 30 mins. Antigen-antibody interaction was visualized using the chromogenic substrate 3,3' diaminobenzidine (DAB) substrate (Proteintech Group, PK10006), and the sections were lightly counterstained with hematoxylin. Immunohistochemistry was evaluated by applying a semi-quantitative Histo-score (H-score) as previously described [22]. The optimal cut off points of USP13, and FHL1 were calculated using X-tile software (Yale University). Under these conditions, samples with H-score <160 and H-score ≥160 were classified as low and high expression of USP13, respectively. Samples with H-score <70 and H-score ≥70 were classified as low and high expression of FHL1, respectively.

Statistical analysis

Data were represented as mean ± standard deviation of 3 independent experiments in *RT-qPCR, CCK-8 and apoptosis detection assay*. Comparison between 2 groups of samples was evaluated using the Student *t* test. The associations between USP13 or FHL1 expression and clinicopathologic parameters were evaluated by Pearson's chi-square test. IC50 value was evaluated via nonlinear regression (curve fit). Probability of differences in overall survival (OS) was ascertained by the Kaplan-Meier method, with a log rank test for significance. Cox proportional hazards regression models were used to analyze the potential independent prognostic factors. Statistical analysis was performed using SPSS 23.0 and GraphPad Prism 6 software.

Results

Expression of USP13 is significantly increased in U2932 cells (Ibrutinib-resistant) compared with WSU-DLCL2 cells (Ibrutinib-sensitive)

First, we examined the mRNA and protein level of USP13 in Ibrutinib-resistant U2932 cells and Ibrutinib-sensitive WSU-DLCL2 cells [4]. Our RT-qPCR data showed that the expression of USP13 mRNA was significantly increased in U2932 cells compared with WSU-DLCL2 cells (**Figure 1A**). Similarly, the protein level of USP13 was also significantly increased in U2932 cells compared with WSU-DLCL2 cells (**Figure 1B**). We then asked whether USP13 protein level was markedly increased upon exposure to Ibrutinib. As shown in **Figure 1C**, increased levels of USP13 were observed in both WSU-DLCL2 and U2932 cells after exposure to Ibrutinib. The activation of the NF-κB signaling pathway was one of the characteristics of the ABC subtype DLBCL and closely related to the emergence of drug resistance. Given that ERK activation was closely related to the activation of the NF-κB signaling pathway and played an important role in drug resistance in DLBCL, and the increased expressions of USP13 and FHL1 were both associated with the activation of the ERK signaling pathway, ERK1/2 phosphorylation after Ibrutinib exposure was assessed. We found that the level of ERK1/2 phosphorylation (pERK1/2: ERK1/2 ratio) was increased in U2932 cells compared with WSU-DLCL2 cells after exposure to Ibrutinib (**Figure 1D**). In addition, the pro-apoptotic Bax protein level was decreased, whereas the anti-apoptotic Bcl-xL protein level was increased in U2932 cells compared with WSU-DLCL2 cells after exposure to Ibrutinib (**Figure 1E**).

USP13 significantly promotes cell growth and decreases Ibrutinib sensitivity in DLBCL

We next established a stable WSU-DLCL2 cell line overexpressing USP13 ($USP13^{OE}$) by lentivirus infections and puromycin selection, and

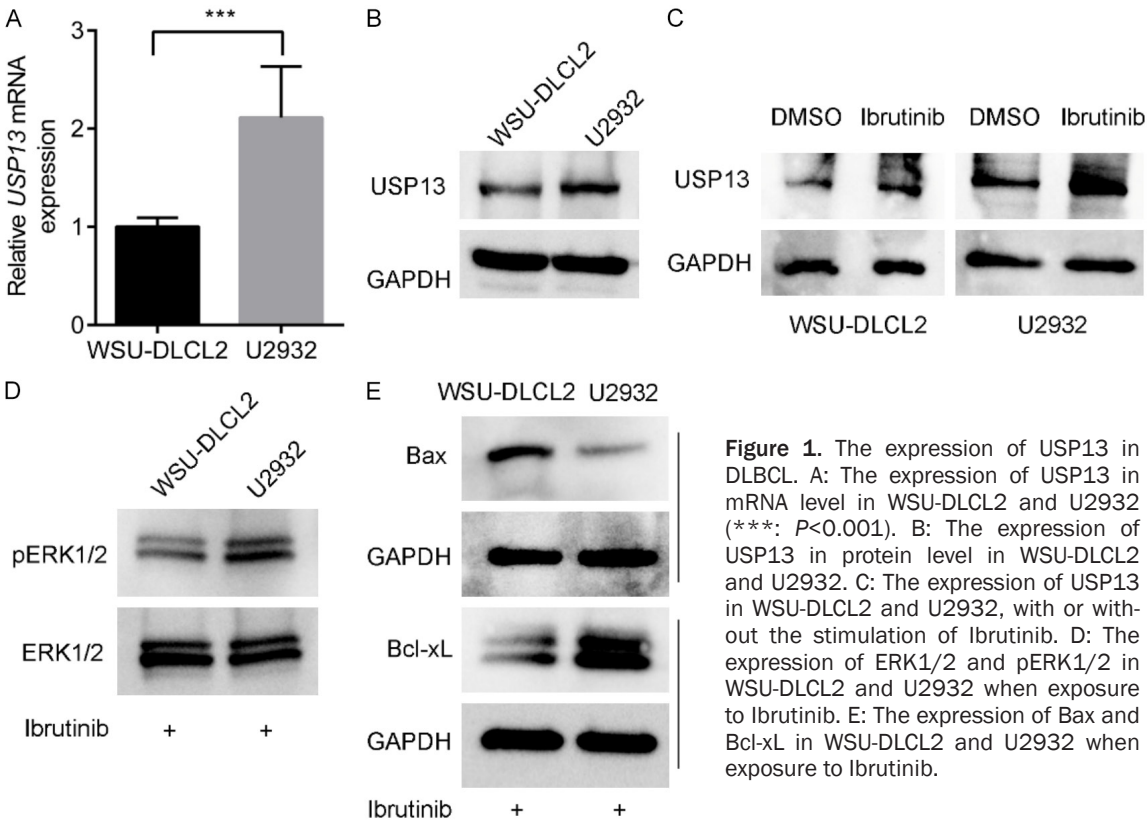

Figure 1. The expression of USP13 in DLBCL. A: The expression of USP13 in mRNA level in WSU-DLCL2 and U2932 (***: P<0.001). B: The expression of USP13 in protein level in WSU-DLCL2 and U2932. C: The expression of USP13 in WSU-DLCL2 and U2932, with or without the stimulation of Ibrutinib. D: The expression of ERK1/2 and pERK1/2 in WSU-DLCL2 and U2932 when exposure to Ibrutinib. E: The expression of Bax and Bcl-xL in WSU-DLCL2 and U2932 when exposure to Ibrutinib.

USP13 levels were confirmed by Western blot (**Figure 2A**). Investigation of USP13 regulation of cell growth indicated that overexpression of USP13 promoted cell growth and increased ERK1/2 phosphorylation in WSU-DLCL2 cells (**Figure 2B** and **2C**). To further validate the role of USP13 in DLBCL cell growth, we next established U2932 cells stable silencing of USP13. As shown in **Figure 2D**, shUSP13#3 was highly effective in depleting USP13 in U2932 cells. As anticipated, USP13 knockdown markedly decreased cell growth and ERK1/2 phosphorylation in U2932 cells (**Figure 2E** and **2F**). As revealed by **Figure 2G**, overexpression of USP13 decreased the response to Ibrutinib. IC50 values for Ibrutinib were 22.32 μM (R^2= 0.9671) for $USP13^{OE}$ cells versus 13.16 μM (R^2=0.9610) for Vector cells (P<0.01). Flow cytometry analysis showed that overexpression of USP13 suppressed Ibrutinib-induced apoptosis in WSU-DLCL2 cells (**Figure 2H**, Supplementary Figure 1A). To confirm this, the effect of ectopic expression of USP13 on Bax and Bcl-xL expression was investigated. Western blot showed that overexpression of USP13 significantly decreased Bax and increased Bcl-xL expression both in the presence or absence of Ibrutinib in WSU-DLCL2 cells (**Figure 2I**). We further tested the effects of USP13 downregulation on Ibrutinib sensitivity. USP13 knockdown sensitized the response to Ibrutinib. IC50 values for Ibrutinib were 11.04 μM (R^2=0.9198) for shUSP13#3 cells versus 19.41 μM (R^2=0.9199) for shCtrl cells (P<0.01, **Figure 2J**). Flow cytometry analysis showed that USP13 knockdown enhanced Ibrutinib-induced apoptosis in U2932 cells (**Figure 2K**, Supplementary Figure 1B). Western blot analysis also revealed that USP13 knockdown increased Bax and decreased Bcl-xL expression both in the presence or absence of Ibrutinib in U2932 cells (**Figure 2L**). These results imply that USP13 may regulate Ibrutinib sensitivity in DLBCL cells.

USP13 inhibitor Spautin-1 sensitizes the response of DLBCL cells to Ibrutinib

We subsequently examined whether Spautin-1, a specific small-molecule inhibitor of USP family members USP10 and USP13, sensitizes the response of DLBCL cells to Ibrutinib. As shown in **Figure 3A** and **3B**, addition of the Spautin-1 resulted in decreased USP13 protein expres-

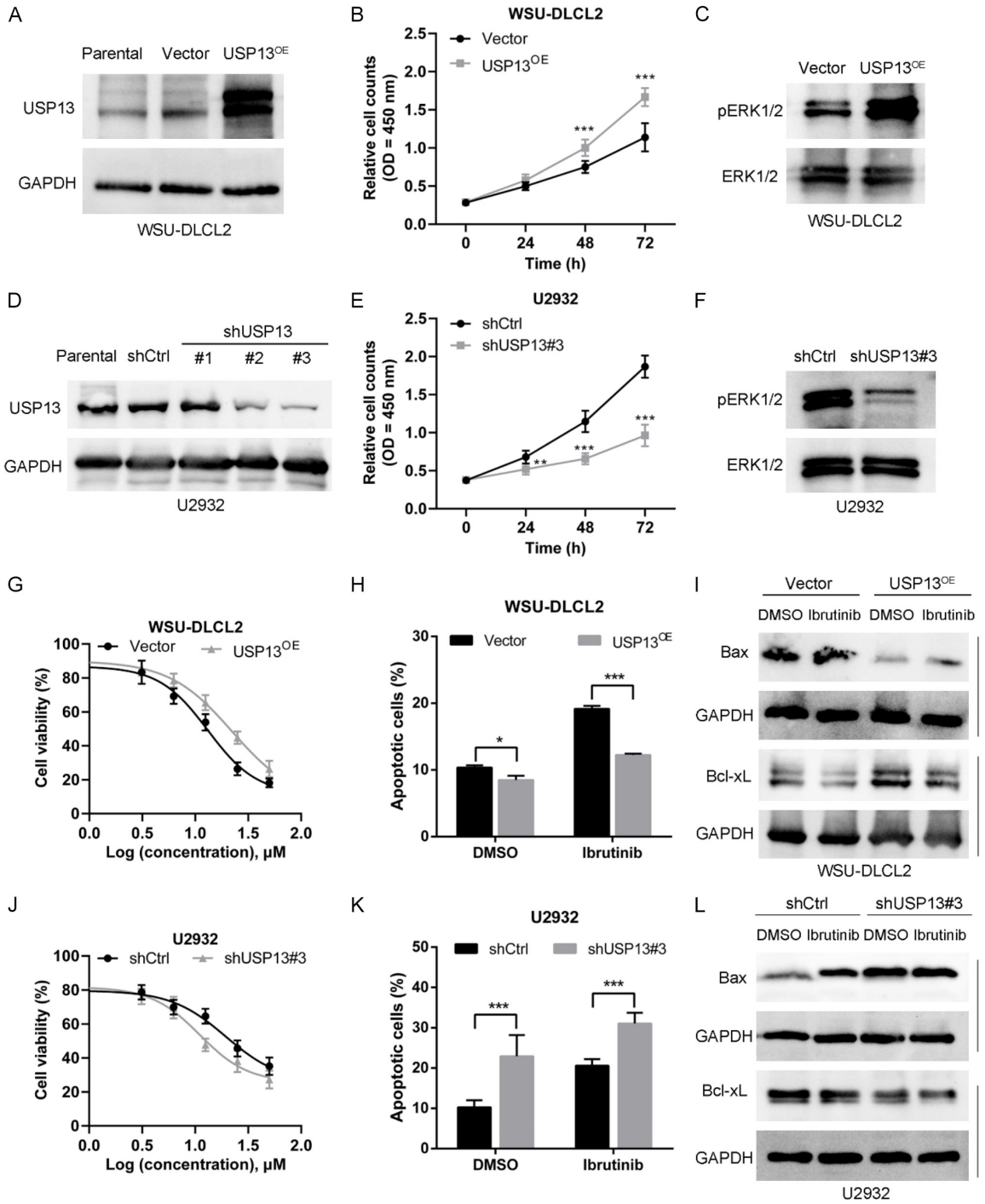

Figure 2. Effect of USP13 on proliferation and apoptosis of DLBCL. A: The efficacy of overexpression of USP13 in WSU-DLCL2 with lentiviral. B: The growth rate of USP13 overexpression (USP13^{OE}) or negative control (Ctrl) WSU-DLCL2 (***: P<0.001). C: The expression of ERK1/2 and pERK1/2 in USP13 overexpression (USP13^{OE}) or negative control (Ctrl) WSU-DLCL2. D: The efficacy of knockdown of USP13 in U2932 with lentiviral. E: The growth rate of USP13 knockdown (shUSP13#3) or negative control (shCtrl) U2932 (**: P<0.01, ***: P<0.001). F: The expression of ERK1/2 and pERK1/2 in USP13 knockdown (shUSP13#3) or negative control (shCtrl) U2932. G: IC50 value of Ibrutinib in USP13 overexpression (USP13^{OE}) or negative control (Ctrl) WSU-DLCL2. H: Apoptosis induced by Ibrutinib in USP13 overexpression (USP13^{OE}) or negative control (Ctrl) WSU-DLCL2 (*: P<0.05, ***: P<0.001). I: The expression of Bax and Bcl-xL induced by Ibrutinib in USP13 overexpression (USP13^{OE}) or negative control (Ctrl) WSU-DLCL2. J: IC50 value of Ibrutinib in USP13 knockdown (shUSP13#3) or negative control (shCtrl) U2932. K: Apoptosis induced by Ibrutinib in USP13 knockdown (shUSP13#3) or negative control (shCtrl) U2932 (***: P<0.001). L: The expression of Bax and Bcl-xL induced by Ibrutinib in USP13 knockdown (shUSP13#3) or negative control (shCtrl) U2932.

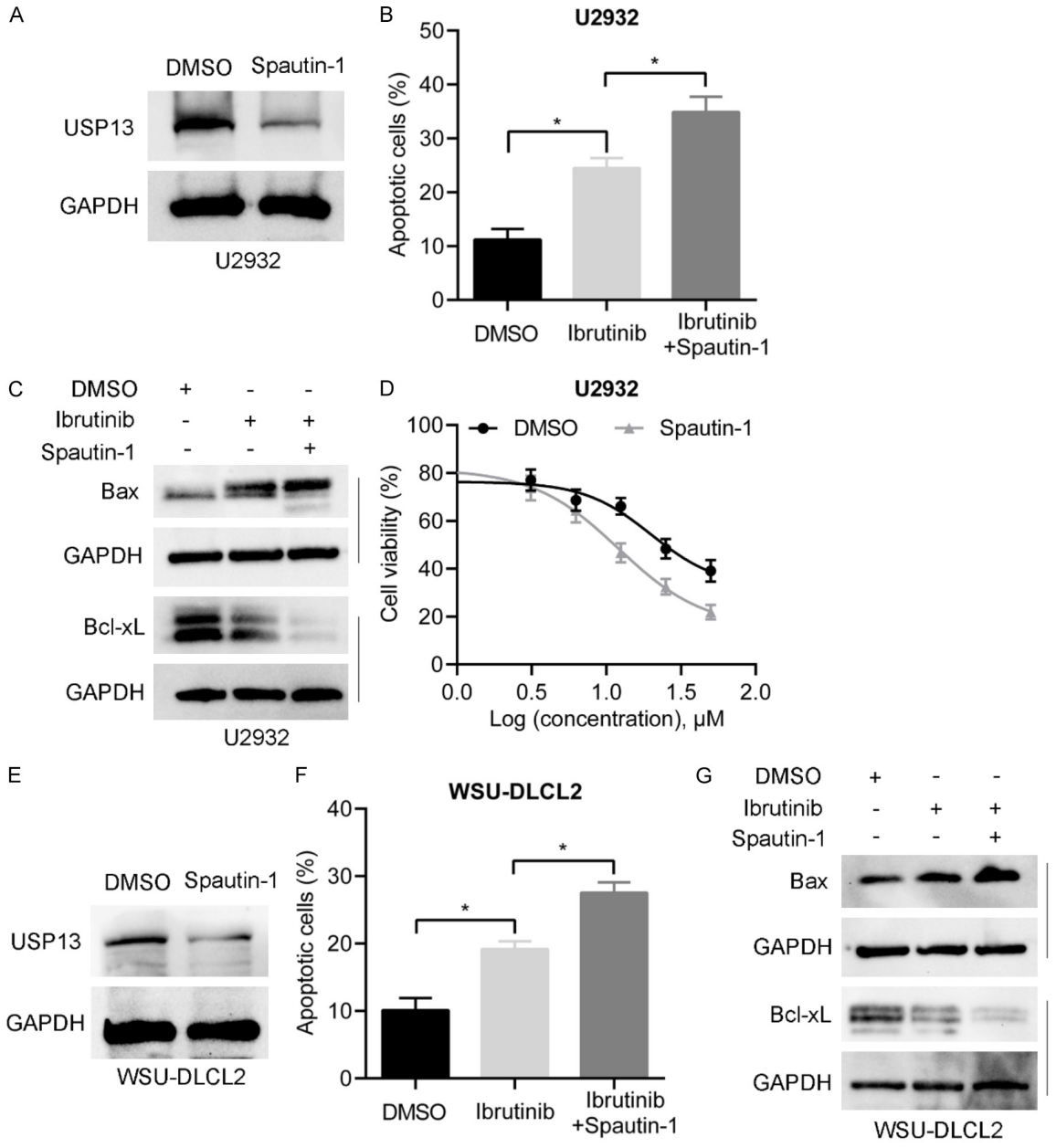

Figure 3. Effect of Spautin-1 on Ibrutinib resistance in DLBCL. A: The efficacy of inhibition of USP13 in U2932 with Spautin-1. B: Apoptosis of U2932 induced by DMSO, Ibrutinib or Ibrutinib and Spautin-1 (*: P<0.05). C: The expression of Bax and Bcl-xL induced by DMSO, Ibrutinib or Ibrutinib and Spautin-1 in U2932. D: IC50 value of Ibrutinib in U2932 with DMSO or Spautin-1. E: The efficacy of inhibition of USP13 in WSU-DLCL2 with Spautin-1. F: Apoptosis of WSU-DLCL2 induced by DMSO, Ibrutinib or Ibrutinib and Spautin-1 (*: P<0.05). G: The expression of Bax and Bcl-xL induced by DMSO, Ibrutinib or Ibrutinib and Spautin-1 in WSU-DLCL2.

sion and enhanced Ibrutinib-induced apoptosis in U2932 cells (Supplementary Figure 1C). Furthermore, Spautin-1 dramatically increased Bax and decreased Bcl-xL expression in the presence of Ibrutinib in U2932 cells (**Figure 3C**). Importantly, Spautin-1 sensitized the response of Ibrutinib-resistant U2932 cells to Ibrutinib. IC50 values for Ibrutinib were 12.05 μM (R^2=0.9588) for Spautin-1-treated cells versus 19.89 μM (R^2=0.9035) for DMSO-treated cells (P<0.001, **Figure 3D**). We further tested whether Spautin-1 could also sensitize the response of WSU-DLCL2 cells to Ibrutinib. Similarly, addition of Spautin-1 also significant-

ly decreased the protein level of USP13 in WSU-DLCL2 cells (**Figure 3E**). In addition, Spautin-1 also enhanced Ibrutinib-induced apoptosis, increased Bax expression and decreased Bcl-xL expression in WSU-DLCL2 cells (**Figure 3F** and **3G**, Supplementary Figure 1D). Taken together, these data suggest that USP13 inhibitor Spautin-1 markedly enhances Ibrutinib-induced apoptosis, and abolishes Ibrutinib resistance in DLBCL cells.

Ectopic expression of USP13 in U2932 cells enhances resistance to Ibrutinib-induced apoptosis, and knockdown of USP13 in WSU-DLCL2 cells increases Ibrutinib-induced apoptosis

We further tested whether ectopic expression of USP13 could enhance resistance to Ibrutinib-induced apoptosis in U2932 cells. We next established USP13^{OE} stable U2932 cells, and USP13 protein expression was confirmed by Western blot (**Figure 4A**). Enforced expression of USP13 increased ERK1/2 phosphorylation, and suppressed Ibrutinib-induced apoptosis in U2932 cells (**Figure 4B** and **4C**, Supplementary Figure 1E). Moreover, overexpression of USP13 significantly decreased Bax and increased Bcl-xL expression both in the presence or absence of Ibrutinib in U2932 cells (**Figure 4D**). We also tested whether downregulation of USP13 could increase Ibrutinib-induced apoptosis in WSU-DLCL2 cells. We next established WSU-DLCL2 cells stable silencing of USP13. As revealed in **Figure 4E**, shUSP13#3 was also highly effective in depleting USP13 in WSU-DLCL2 cells. As anticipated, USP13 knockdown dramatically suppressed ERK1/2 phosphorylation, and increased Ibrutinib-induced apoptosis in WSU-DLCL2 cells (**Figure 4F** and **4G**, Supplementary Figure 1F). As shown in **Figure 4H**, USP13 knockdown increased Bax and decreased Bcl-xL expression both in the presence or absence of Ibrutinib in WSU-DLCL2 cells.

USP13 interacted with FHL1 and stabilized the expression of FHL1 via deubiquitination

To identify USP13-interacting proteins, we performed immunoprecipitation-mass spectrometry (IP-MS) analysis. Our IP-MS data showed that FHL1 was among the group of USP13-interacting proteins in both WSU-DLCL2 and U2932, it was also reported to be related to the formation of tumor drug resistance. In addition, FHL1 has been reported to be regulated by post-translational modifications such as ubiquitination. Therefore, we proposed a hypothesis that USP13 played a role in drug resistance through FHL1 in DLBCL. We next determined the interaction between USP13 and FHL1 in WSU-DLCL2 and U2932 cells at an endogenous protein level. Co-IP/Western blot assays further confirmed the interaction between USP13 and FHL1 (**Figure 5A**). Next, we co-transfected exogenous USP13 and FHL1 into the HEK293T cells. The interaction between USP13 and FHL1 was verified by employing exogenous Co-IP tests HEK293T cells, suggesting that there was indeed interaction between USP13 and FHL1 (**Figure 5B**). Western blot analysis showed that overexpression of USP13 in WSU-DLCL2 and U2932 significantly enhanced the expression of FHL1 in the absence and presence of Ibrutinib in WSU-DLCL2 and U2932 cells. In contrast, knockdown of USP13 in WSU-DLCL2 and U2932 decreased the expression of FHL1 in the absence and presence of Ibrutinib (**Figure 5C**). Overexpression of USP13 decreased ubiquitination of FHL1 and stabilized FHL1 protein (**Figure 5D** and **5E**). Taken together, these data suggest that USP13 can interact with FHL1 and stabilize the expression of FHL1 via deubiquitination.

Knockdown of FHL1 in DLBCL cells increases Ibrutinib-induced apoptosis

We next established U2932 cells stable silencing of FHL1. As shown in **Figure 6A**, shFHL1 was highly effective in depleting FHL1 expression in U2932 cells. FHL1 knockdown significantly suppressed ERK1/2 phosphorylation in U2932 cells (**Figure 6B**). FHL1 knockdown increased Ibrutinib-induced apoptosis in U2932 cells (**Figure 6C**, Supplementary Figure 2A). Moreover, knockdown of FHL1 increased Bax and decreased Bcl-xL expression in U2932 cells (**Figure 6D**). We next determined whether knockdown of FHL1 in WSU-DLCL2 cells increases Ibrutinib-induced apoptosis. We established WSU-DLCL2 cells stable silencing of FHL1. As shown in **Figure 6E**, shFHL1 was also proven to be highly effective in depleting FHL1 expression in WSU-DLCL2 cells. Similar results were observed after silencing of FHL1 in WSU-DLCL2 cells (**Figure 6F-H**, Supplementary Figure 2B). Collectively, the above findings suggest that knockdown of FHL1 increases Ibrutinib-induced apoptosis in DLBCL cells.

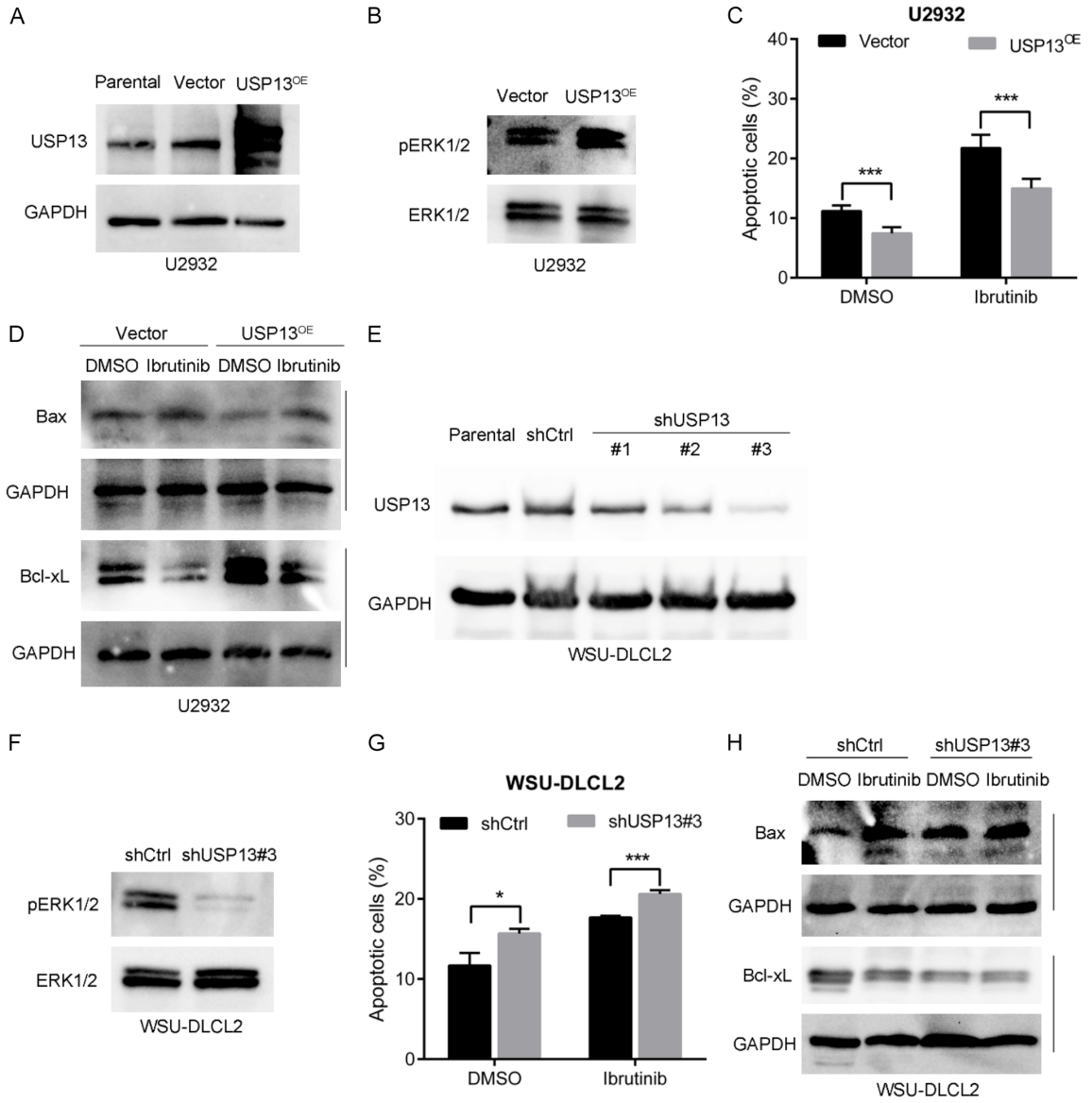

Figure 4. Effect of overexpression of USP13 on apoptosis of Ibrutinib-resistant U2932 and downregulation of USP13 on apoptosis of Ibrutinib-sensitive WSU-DLCL2. A: The efficacy of overexpression of USP13 in U2932 with lentiviral. B: The expression of ERK1/2 and pERK1/2 in USP13 overexpression (USP13^{OE}) or negative control (Ctrl) U2932. C: Apoptosis induced by Ibrutinib in USP13 overexpression (USP13^{OE}) or negative control (Ctrl) U2932 (***: P<0.001). D: The expression of Bax and Bcl-xL induced by Ibrutinib in USP13 overexpression (USP13^{OE}) or negative control (Ctrl) U2932. E: The efficacy of knockdown of USP13 in WSU-DLCL2 with lentiviral. F: The expression of ERK1/2 and pERK1/2 in USP13 knockdown (shUSP13#3) or negative control (shCtrl) WSU-DLCL2. G: Apoptosis induced by Ibrutinib in USP13 knockdown (shUSP13#3) or negative control (shCtrl) WSU-DLCL2 (*: P<0.05, ***: P<0.001). H: The expression of Bax and Bcl-xL induced by Ibrutinib in USP13 knockdown (shUSP13#3) or negative control (shCtrl) WSU-DLCL2.

USP13 mediated drug resistance is reversed by inhibition of FHL1 in DLBCL cells

We subsequently determined whether USP13 mediated drug resistance could be reversed by inhibition of FHL1 in DLBCL cells. Knockdown of FHL1 by infection of FHL1 lentivirus decreased FHL1 expression in USP13^{OE}-U2932 and WSU-DLCL2 cells (**Figure 7A**). As shown in **Figure 7B**, FHL1 knockdown significantly suppressed ERK1/2 phosphorylation in USP13^{OE}-U2932 and WSU-DLCL2 cells. FHL1 knockdown increased apoptosis in USP13^{OE}-U2932 and WSU-DLCL2 cells (**Figure 7C** and **7D**,

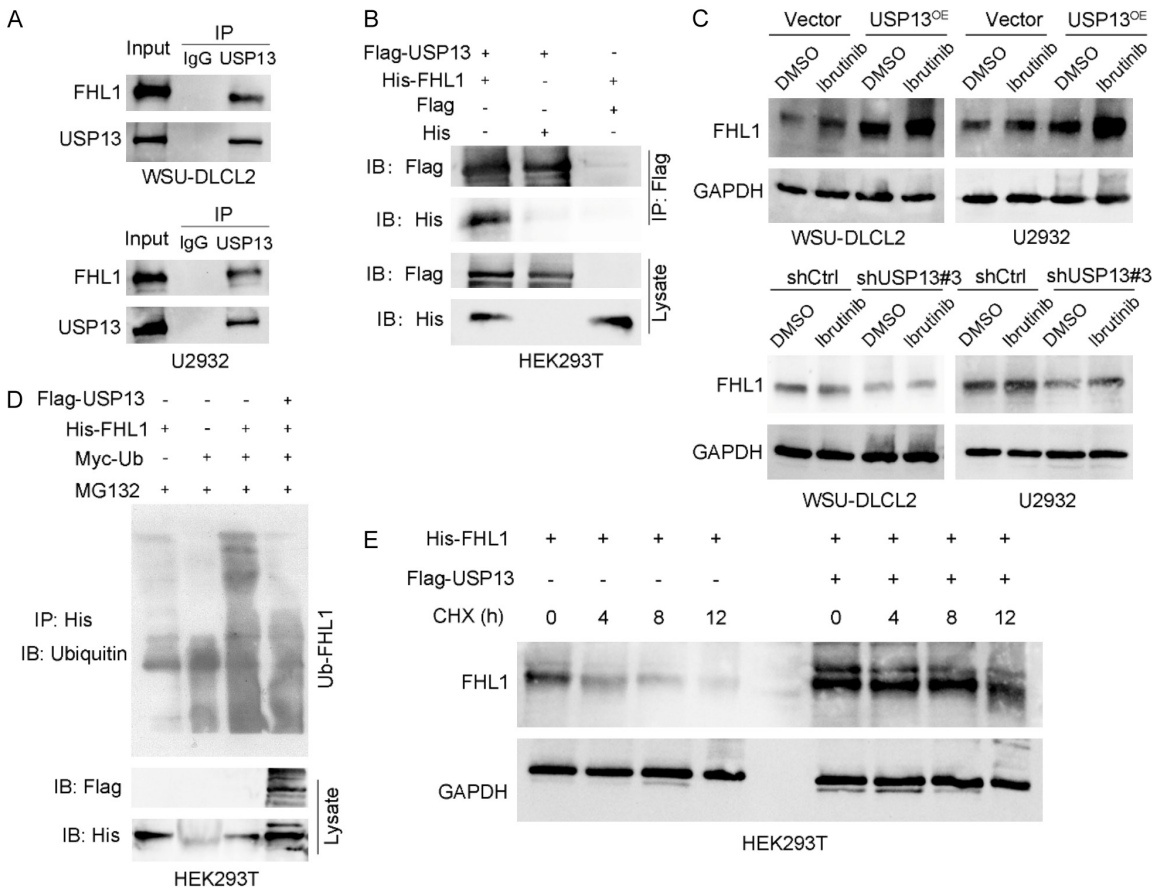

Figure 5. USP13 positively regulated the expression of FHL1 through deubiquitination. A: The interaction between USP13 and FHL1 in WSU-DLCL2 and U2932. B: The interaction between USP13 and FHL1 in HEK293T. C: The expression of FHL1 induced by Ibrutinib in USP13 overexpression ($USP13^{OE}$) or negative control (Ctrl) and USP13 knockdown (shUSP13#3) or negative control (shCtrl) WSU-DLCL2 and U2932. D: Ubiquitination level FHL1 in HEK293T with or without USP13. E: Expression level of FHL1 in HEK293T with or without USP13 in the case of exposure to CHX for 0, 4, 8 or 12 h.

Supplementary Figure 3). Further, knockdown of FHL1 reversed the decrease of Bax and increase of Bcl-xL induced by USP13 overexpression in U2932 and WSU-DLCL2 cells (**Figure 7E** and **7F**). These data suggest that FHL1 knockdown reverses USP13 mediated Ibrutinib resistance *in DLBCL cells*.

Expression of USP13 and FHL1 in DLBCL patients

Expression analysis of USP13 and FHL1 was conducted with primary tumors from 181 DLBCL patients by immunohistochemistry. USP13 was highly expressed in 67 patients (H-score >160), and low expressed in 114 cases (H-score ≤160). FHL1 was highly expressed in 39 patients (H-score >70), and low expressed in 142 patients (H-score ≤70) (Supplementary Figure 4). As shown in **Table 1**, USP13 expression status was correlated with age (P=0.010), B symptoms (P=0.038), ECOG PS score (P=0.006), IPI score (P=0.021) and serum LDH level (P=0.005). However, there was no significant correlation between the expression of FHL1 and the clinicopathological parameters (all P>0.05). Kaplan-Meier survival analysis showed that overall survival (OS) was significantly prolonged in patients with low USP13 expression (P=0.001), while there was no significant correlation between the expression level of FHL1 and OS (P=0.255) (**Figure 8A**, **8B**). When combined USP13 with FHL1 expression, we found that there was a trend toward shortened OS in the subset of patients with high expression of both USP13 and FHL1, but

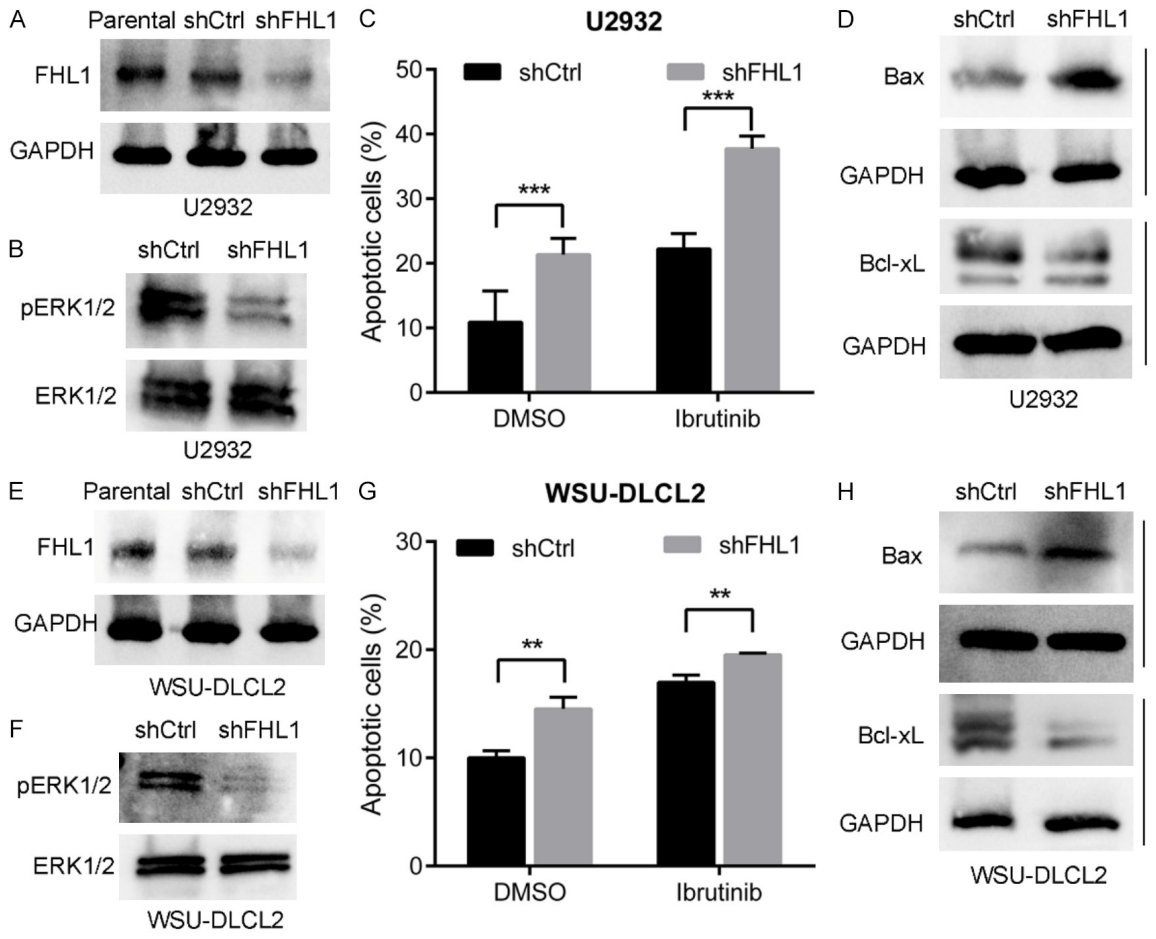

Figure 6. Effect of FHL1 on Ibrutinib-induced apoptosis of DLBCL. A: The efficacy of knockdown of FHL1 in U2932 with lentiviral. B: The expression of ERK1/2 and pERK1/2 in FHL1 knockdown (shFHL1) or negative control (shCtrl) U2932. C: Apoptosis induced by Ibrutinib in FHL1 knockdown (shFHL1) or negative control (shCtrl) U2932 (***: $P<0.001$). D: The expression of Bax and Bcl-xL in FHL1 knockdown (shFHL1) or negative control (shCtrl) U2932. E: The efficacy of knockdown of FHL1 in WSU-DLCL2 with lentiviral. F: The expression of ERK1/2 and pERK1/2 in FHL1 knockdown (shFHL1) or negative control (shCtrl) WSU-DLCL2. G: Apoptosis induced by Ibrutinib in FHL1 knockdown (shFHL1) or negative control (shCtrl) WSU-DLCL2 (**: $P<0.01$). H: The expression of Bax and Bcl-xL in FHL1 knockdown (shFHL1) or negative control (shCtrl) WSU-DLCL2.

there was no statistically significant difference ($P=0.126$, **Figure 8C**). Further analysis showed that in patients with Ki-67 index lower than 75%, patients with high expression of both USP13 and FHL1 had shortened OS than other patients ($P=0.003$, **Figure 8D**). In patients with involvement of <2 extranodal sites, patients with high expression of both USP13 and FHL1 had shortened OS than other patients ($P=0.015$, **Figure 8E**). In patients with ECOG PS score <2, patients with high expression of both USP13 and FHL1 also had shortened OS than other patients ($P=0.008$, **Figure 8F**). Cox analysis results suggested that age ($P<0.001$), Hans classification ($P=0.010$), B symptoms ($P<0.001$), extranodal invasion ($P=0.015$), ECOG PS score ($P<0.001$), IPI score ($P<0.001$), serum LDH level ($P<0.001$) and USP13 expression ($P=0.006$) were correlated with OS. Statistically significant variables in the Cox univariate analysis were included in the multivariate analysis. Multivariate analysis show that IPI score ($P<0.001$), Hans classification ($P=0.011$) and USP13 expression ($P=0.043$) are independent prognostic factors for OS (**Table 2**).

Discussion

DLBCL is the most common type of non-Hodgkin lymphoma. The formation of tumor resis-

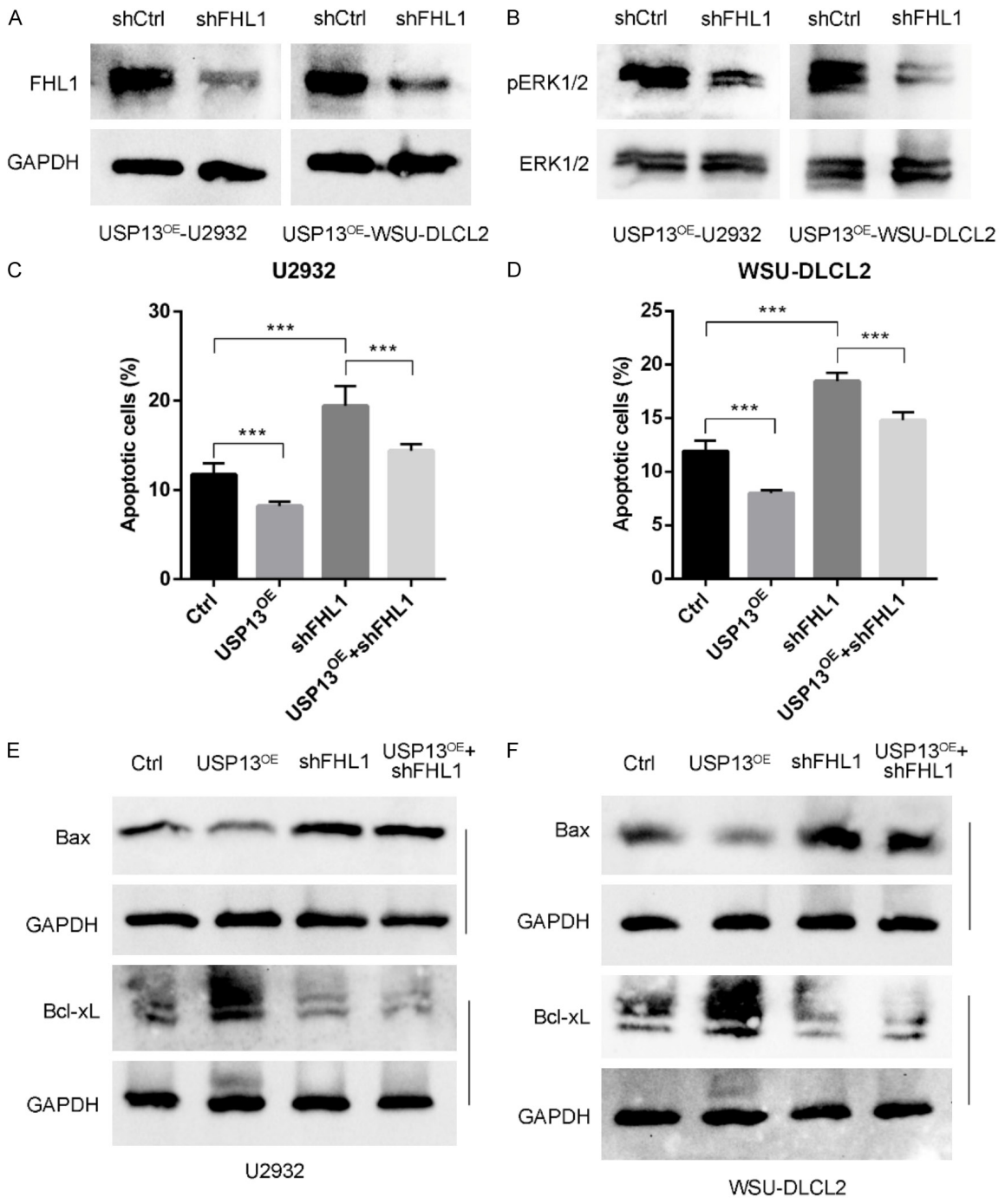

Figure 7. USP13 affects Ibrutinib-induced apoptosis of DLBCL through FHL1. A: The efficacy of knockdown of FHL1 in USP13-overexpressed U2932 and WSU-DLCL2 with lentiviral. B: The expression of ERK1/2 and pERK1/2 in FHL1 knockdown (shFHL1) or negative control (shCtrl) USP13 overexpressed U2932 and WSU-DLCL2. C: Apoptosis in negative control (Ctrl), USP13 overexpression ($USP13^{OE}$), FHL1 knockdown (shFHL1) or USP13 overexpression plus FHL1 knockdown ($USP13^{OE}$+shFHL1) U2932 (***: $P<0.001$). D: Apoptosis in negative control (Ctrl), USP13 overexpression ($USP13^{OE}$), FHL1 knockdown (shFHL1) or USP13 overexpression plus FHL1 knockdown ($USP13^{OE}$+shFHL1) WSU-DLCL2 (***: $P<0.001$). E: The expression of Bax and Bcl-xL in negative control (Ctrl), USP13 overexpression ($USP13^{OE}$), FHL1 knockdown (shFHL1) or USP13 overexpression plus FHL1 knockdown ($USP13^{OE}$+shFHL1) U2932. F: The expression of Bax and Bcl-xL in negative control (Ctrl), USP13 overexpression ($USP13^{OE}$), FHL1 knockdown (shFHL1) or USP13 overexpression plus FHL1 knockdown ($USP13^{OE}$+shFHL1) WSU-DLCL2.

Table 1. Relationship between USP13 and FHL1 expression levels and clinicopathological features of 181 patients with DLBCL

Clinicopathological parameter	*n*	USP13		*P* value	FHL1		*P* value
		Low	High		Low	High	
Age				0.010			0.419
<60	56	43	13		46	10	
≥60	125	71	54		96	29	
Gender				0.331			0.306
male	78	46	32		64	14	
female	103	68	35		78	25	
Hans classification[a]				0.707			0.802
GCB	43	28	15		33	10	
non-GCB	126	78	48		99	27	
B symptom				0.038			0.288
exist	158	104	54		122	36	
absence	23	10	13		20	3	
Ki-67[b]				0.521			0.540
<75%	63	41	22		51	12	
≥75%	113	68	45		87	26	
Extranodal invasion				0.647			0.113
0-1	115	71	44		86	29	
≥2	66	43	23		56	10	
ECOG PS score				0.006			0.614
<2	105	75	30		81	24	
≥2	76	39	37		61	15	
IPI score				0.021			0.450
0-2	74	54	20		56	18	
3-5	107	60	47		86	21	
LDH				0.005			0.630
normal	52	41	11		42	10	
high	129	73	56		100	29	

Annotation: [a]12 value were missing in Hans classification; [b]5 value were missing in Ki67 value.

tance is one of the key factors that make DLBCL difficult to treat or eventually relapse. Currently, the standard treatment for DLBCL is R-CHOP, but numerous patients fail to achieve remission or eventually relapse, especially ABC subtype. The reason of drug resistance to R-CHOP may be related to abnormal DNA repair, altered epigenetic modification, altered drug metabolism and abnormal immune microenvironment. For instance, the treatment effect of R-CHOP is better in patients with high expression of CD24 [23]. At the same time, TCFL5 induces resistance to adriamycin through interaction with GPX4, aberrant DNA methylation also induces resistance to R-CHOP regimens [24].

In recent years, in order to solve the problem of drug resistance to R-CHOP treatment regimen and improve the therapeutic effect of DLBCL patients, a variety of new therapies have been developed. These drugs can be mainly divided into signaling pathway inhibitors, anti-angiogenesis drugs, immune checkpoint related drugs, anti-immune escape drugs, BTK inhibitor and other new targeted therapeutic drugs, which includes Ibrutinib, but there are still patients who are resistant to treatment.

The prognosis of the ABC subtype of DLBCL is poor. Activation of the BTK and its downstream NF-κB signaling pathway is one of the characteristics of the ABC subtype of DLBCL. Ibrutinib, as a potent BTK inhibitor that blocks the BCR-dependent NF-κB signaling pathway, can lead

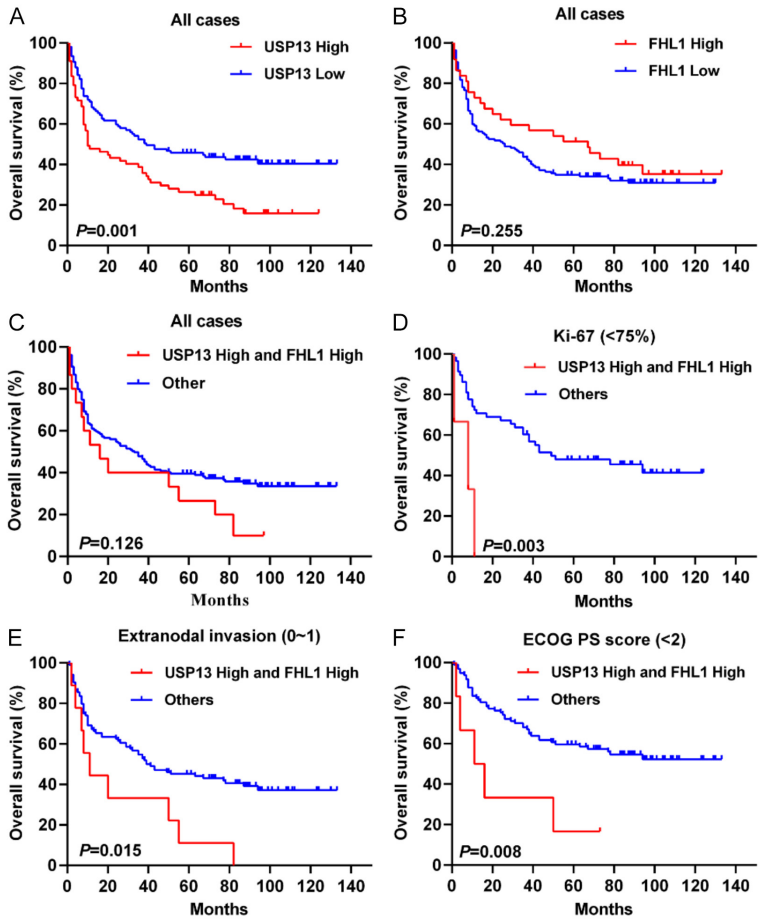

Figure 8. Expression of USP13 and FHL1 in DLBCL patients. A: Survival curve was drawn according to the expression level of USP13 in tumor tissues of patients, and OS was significantly prolonged in patients with low USP13 expression. B: Survival curves were drawn according to the expression level of FHL1 in tumor tissues of patients, and there was no significant correlation between the expression status of FHL1 and patients' OS. C: Survival curves were drawn based on the expression levels of USP13 and FHL1 in the tumor tissues of 181 patients. D: In patients whose Ki-67 index in tumor tissue lower than 75%, the survival curve was drawn according to the expression levels of USP13 and FHL1 in the tumor tissue. E: In patients with extrannodal tumor invasion less than 2 places, the survival curve was drawn according to the expression levels of USP13 and FHL1 in the tumor tissue of the patients. F: In patients whose ECOG PS score <2, survival curves were plotted according to the expression levels of USP13 and FHL1 in tumor tissue.

to remission in about 40% patients with ABC subtype. At present, Ibrutinib has been approved for the treatment of chronic lymphocytic leukemia, mantle cell lymphoma and other hematologic malignancies, and a number of phase I clinical trials of Ibrutinib for the treatment of relapsed/refractory DLBCL are also underway.

However, there are still cases of resistance to Ibrutinib. Studies have shown that the elevation of CD79B, 17p deletion, the decline of PTEN and FOXO3a, the up-regulation of BCL2 and PIMA1 are closely related to Ibrutinib resistance [25]. Down-regulation of XBP1 leads to down-regulation of UPR, which mediates Ibrutinib resistance. Mutations in PLCγ2, MYD88, C481S in BTK are also associated with Ibrutinib resistance [25]. Although Ibrutinib effectively inhibits the kinase activity of BTK, studies have shown that NF-κB and other downstream signaling pathway are activated in DLBCL when BTK is inhibited. However, the mechanism of resistance to Ibrutinib in DLBCL has not been fully elucidated.

The NF-κB pathway is activated in patients with ABC subtype, and many components of this pathway undergo post-translational modifications [26]. Post-translational modification plays an important role in mediating drug resistance in patients with ABC subtype. Therapy targeting post-translational modification is also an effective strategy to overcome drug resistance in tumor. Deubiquitination is an important way of post-translational modification. As a deubiquitinating enzyme, USP13 plays an important role in mediating drug resistance in tumors. USP13 mainly mediates tumor resistance through its deubiquitination enzyme activity. For instance, USP13 binds to mutant EGFR through UBA domain, inhibits the degradation of mutant EGFR by deubiquitination, and mediates afatinib resistance in non-small cell lung cancer. USP13 also induces imatinib resistance in gastrointestinal stromal tumors through interacting with autophagy-related protein 5 and down-regulating its ubiquitination levels. In addition, USP13 deubiquitinates RAP80 by interacting with RAP80 to form the RAP80-BRCA1 complex,

Table 2. Cox univariate and multivariate regression analysis

Variate	OS	*P* value
	HR (95% CI)	
Cox unifactor analysis		
Age (≥60 *vs* <60)	2.290 (1.482-3.537)	<0.001
Gender (male *vs* female)	1.010 (0.706-1.444)	0.959
Hans classification (nonGCB *vs* GCB)	1.870 (1.163-3.007)	0.010
B symptom (exist *vs* absence)	2.373 (1.462-3.853)	<0.001
Ki-67 (≥75% *vs* <75%)	1.418 (0.961-2.093)	0.079
Extranodal invasion (≥2 *vs* 0-1)	1.572 (1.093-2.259)	0.015
ECOG PS score (≥2 *vs* <2)	4.325 (2.983-6.272)	<0.001
IPI score (3-5 vs 0-2)	3.614 (2.399-5.444)	<0.001
LDH (high vs normal)	3.271 (2.035-5.257)	<0.001
USP13 (high vs low)	1.653 (1.155-2.367)	0.006
FHL1 (high vs low)	0.817 (0.526-1.269)	0.368
Cox multivariate analysis		
IPI score (3-5 vs 0-2)	3.060 (2.002-4.678)	<0.001
B symptom (exist *vs* absence)	1.534 (0.894-2.633)	0.120
Hans classification (nonGCB *vs* GCB)	1.864 (1.155-3.007)	0.011
USP13 (high *vs* low)	1.484 (1.013-2.175)	0.043

which regulates DNA damage response and induces chemotherapy resistance in ovarian cancer patients.

In this paper, we found that post-translational modification plays a very important role in Ibrutinib resistance in DLBCL. The expression of USP13 was higher in Ibrutinib-resistant U2932 cells then Ibrutinib-sensitive WSU-DLCL2 cells. Ibrutinib exposure also increased USP13 expression in DLBCL cells. High expression of USP13 promoted the proliferation of DLBCL cells, inhibited the apoptosis induced by Ibrutinib, and decreased its sensitivity to Ibtutinib. Immunoprecipitation results showed that USP13 and FHL1 interacted. FHL1 is a cytoskeletal protein whose expression could be regulated by post-translational modifications such as ubiquitination. Our results showed that the increased expression of USP13 stabilized the expression of cytoskeleton molecule FHL1 through deubiquitination modification, thereby mediating the activation of ERK signaling pathway to inhibit Ibrutinib-induced apoptosis. ERK activation is closely related to the activation of NF-κB signaling pathway, which plays an important role in drug resistance in DLBCL. Our study illustrated the important role of USP13-FHL1-ERK signaling pathway in mediating Ibrutinib resistance in DLBCL.

In addition, hematologic tumors apply mitochondrial apoptosis mechanisms to survive by overexpressing anti-apoptotic Bcl-2 family proteins [27]. Our results confirmed that USP13-FHL1 interaction caused a decrease in the expression of pro-apoptotic protein Bax and an increase in the expression of anti-apoptotic protein Bcl-xL, thereby exerting an anti-apoptotic effect and causing resistance to Ibrutinib.

Both USP13 and FHL1 are promising targets for tumor therapy, but the role of their interaction in mediating treatment resistance have been rarely reported. In this paper, we detected the relationship between the expression of USP13/FHL1 and apoptosis-related protein Bax and Bcl-xL in DLBCL, which provided a new way to solve the problem of Ibrutinib resistance in patients with ABC subtype DLBCL. The results of immunohistochemical staining also suggested that the expression level of USP13 in DLBCL was closely related to the prognosis of patients. Patients with low USP13 expression in tumor tissue had longer OS than those with high USP13 expression, which could be used to predict the prognosis of patients.

Paraffin tissue samples from DLBCL patients who were treated with BTK inhibitors (Ibrutinib or Zanubrutinib) were also collected for immunohistochemical staining. The results suggested that patients with low USP13 expression were more likely to benefit from BTK inhibitor therapy. However, due to the limited number of patients treated with BTK inhibitors, we will further verify this conclusion by expanding the sample size.

Acknowledgements

This work was supported by the Natural Science Foundation of Nantong (grant no. JC2023038).

Disclosure of conflict of interest

None.

Address correspondence to: Xiaobing Miao and Song He, Department of Pathology, Affiliated Tumor Hospital of Nantong University, No. 30, Tongyang North Road, Nantong 226361, Jiangsu, China. E-mail: miaoxiaobing@ntu.edu.cn (XBM); ntzlyyhesong515@ntu.edu.cn (SH)

References

[1] Alsaadi M, Khan MY, Dalhat MH, Bahashwan S, Khan MU, Albar A, Almehdar H and Qadri I. Dysregulation of miRNAs in DLBCL: causative factor for pathogenesis, diagnosis and prognosis. Diagnostics (Basel) 2021; 11: 1739.

[2] Battistello E, Katanayeva N, Dheilly E, Tavernari D, Donaldson MC, Bonsignore L, Thome M, Christie AL, Murakami MA, Michielin O, Ciriello G, Zoete V and Oricchio E. Pan-SRC kinase inhibition blocks B-cell receptor oncogenic signaling in non-Hodgkin lymphoma. Blood 2018; 131: 2345-2356.

[3] Yu X, Wang X, Wang X, Zhou Y, Li Y, Wang A, Wang T, An Y, Sun W, Du J, Tong X and Wang Y. TEOA inhibits proliferation and induces DNA damage of diffuse large B-cell lymphoma cells through activation of the ROS-dependent p38 MAPK signaling pathway. Front Pharmacol 2020; 11: 554736.

[4] Paul J, Soujon M, Wengner AM, Zitzmann-Kolbe S, Sturz A, Haike K, Keng Magdalene KH, Tan SH, Lange M, Tan SY, Mumberg D, Lim ST, Ziegelbauer K and Liu N. Simultaneous inhibition of PI3Kdelta and PI3Kalpha induces ABC-DLBCL regression by blocking BCR-dependent and -independent activation of NF-kappaB and AKT. Cancer Cell 2017; 31: 64-78.

[5] Wilson WH, Young RM, Schmitz R, Yang Y, Pittaluga S, Wright G, Lih CJ, Williams PM, Shaffer AL, Gerecitano J, de Vos S, Goy A, Kenkre VP, Barr PM, Blum KA, Shustov A, Advani R, Fowler NH, Vose JM, Elstrom RL, Habermann TM, Barrientos JC, McGreivy J, Fardis M, Chang BY, Clow F, Munneke B, Moussa D, Beaupre DM and Staudt LM. Targeting B cell receptor signaling with ibrutinib in diffuse large B cell lymphoma. Nat Med 2015; 21: 922-926.

[6] Joseph RE, Amatya N, Fulton DB, Engen JR, Wales TE and Andreotti A. Differential impact of BTK active site inhibitors on the conformational state of full-length BTK. Elife 2020; 9: e60470.

[7] Wang Y and Wang F. Post-translational modifications of deubiquitinating enzymes: expanding the ubiquitin code. Front Pharmacol 2021; 12: 685011.

[8] Akutsu M, Dikic I and Bremm A. Ubiquitin chain diversity at a glance. J Cell Sci 2016; 129: 875-880.

[9] Talreja J, Bauerfeld C, Wang X, Hafner M, Liu Y and Samavati L. MKP-1 modulates ubiquitination/phosphorylation of TLR signaling. Life Sci Alliance 2021; 4: e202101137.

[10] Liu X and Moussa C. Regulatory role of ubiquitin specific protease-13 (USP13) in misfolded protein clearance in neurodegenerative diseases. Neuroscience 2021; 460: 161-166.

[11] Ren H, Mu W and Xu Q. miR-19a-3p inhibition alleviates sepsis-induced lung injury via enhancing USP13 expression. Acta Biochim Pol 2021; 68: 201-206.

[12] Morgan EL, Patterson MR, Barba-Moreno D, Scarth JA, Wilson A and Macdonald A. The deubiquitinase (DUB) USP13 promotes Mcl-1 stabilisation in cervical cancer. Oncogene 2021; 40: 2112-2129.

[13] Biterge Sut B. Molecular profiling of immune cell-enriched severe acute respiratory syndrome coronavirus 2 (SARS-CoV-2) interacting protein USP13. Life Sci 2020; 258: 118170.

[14] Antao AM, Kaushal K, Das S, Singh V, Suresh B, Kim KS and Ramakrishna S. USP48 governs cell cycle progression by regulating the protein level of aurora B. Int J Mol Sci 2021; 22: 8508.

[15] Wu Y, Zhang Y, Liu C, Zhang Y, Wang D, Wang S, Wu Y, Liu F, Li Q, Liu X, Zaky MY, Yan D and Liu S. Amplification of USP13 drives non-small cell lung cancer progression mediated by AKT/MAPK signaling. Biomed Pharmacother 2019; 114: 108831.

[16] Man X, Piao C, Lin X, Kong C, Cui X and Jiang Y. USP13 functions as a tumor suppressor by blocking the NF-kB-mediated PTEN downregulation in human bladder cancer. J Exp Clin Cancer Res 2019; 38: 259.

[17] Li Y, Pu G, Chen C and Yang L. Inhibition of FHL1 inhibits cigarette smoke extract-induced proliferation in pulmonary arterial smooth muscle cells. Mol Med Rep 2015; 12: 3801-3808.

[18] Sun L, Chen L, Zhu H, Li Y, Chen CC and Li M. FHL1 promotes glioblastoma aggressiveness through regulating EGFR expression. FEBS Lett 2021; 595: 85-98.

[19] Song J, Liang K, Wei T, Li L, Huang Z, Chen G, Mao N and Yang J. Expression and predictive significance of FHL1 and SLIT3 in surgically resected lung adenocarcinoma. Comb Chem High Throughput Screen 2023; 26: 2226-2237.

[20] Xu X, Fan Z, Liang C, Li L, Wang L, Liang Y, Wu J, Chang S, Yan Z, Lv Z, Fu J, Liu Y, Jin S, Wang T, Hong T, Dong Y, Ding L, Cheng L, Liu R, Fu S, Jiao S and Ye Q. A signature motif in LIM proteins mediates binding to checkpoint proteins and increases tumour radiosensitivity. Nat Commun 2017; 8: 14059.

[21] Zhou L, Ding L, Liu J, Zhang Y, Luo X, Zhao L and Ren J. Four-and-a-half LIM protein 1 promotes paclitaxel resistance in hepatic carcinoma cells through the regulation of caspase-3 activation. J Cancer Res Ther 2018; 14 Suppl: S767-S773.
[22] She L, Zhang X, Shen R, He S and Miao X. Expression and role of FKBPL in lung adenocarcinoma. J Cancer 2024; 15: 166-175.
[23] Qiao LY, Li HB, Zhang Y, Shen D, Liu P and Che YQ. CD24 contributes to treatment effect in ABC-DLBCL patients with R-CHOP resistance. Pharmgenomics Pers Med 2021; 14: 591-599.
[24] Lu X, Zhang Q and Xie Y. TCFL5 knockdown sensitizes DLBCL to doxorubicin treatment via regulation of GPX4. Cell Signal 2023; 110: 110831.
[25] Zhang XT, Hu XB, Wang HL, Kan WJ, Xu L, Wang ZJ, Xiang YQ, Wu WB, Feng B, Li JN, Gao AH, Dong TC, Xia CM, Zhou YB and Li J. Activation of unfolded protein response overcomes Ibrutinib resistance in diffuse large B-cell lymphoma. Acta Pharmacol Sin 2021; 42: 814-823.
[26] Yu X, Li W, Deng Q, LIU H, Wang X, Hu H, Cao Y, Xu-Monette ZY, Li L, Zhang M, LU Z, Young K and Li Y. MYD88 L265P elicits mutation-specific ubiquitination to drive NF-κB activation and lymphomagenesis. Blood 2021; 137: 1615-1627.
[27] Boiko S, Proia T, San Martin M, Gregory GP, Wu MM, Aryal N, Hattersley M, Shao W, Saeh JC, Fawell SE, Johnstone RW, Drew L and Cidado J. Targeting Bfl-1 via acute CDK9 inhibition overcomes intrinsic BH3-mimetic resistance in lymphomas. Blood 2021; 137: 2947-2957.

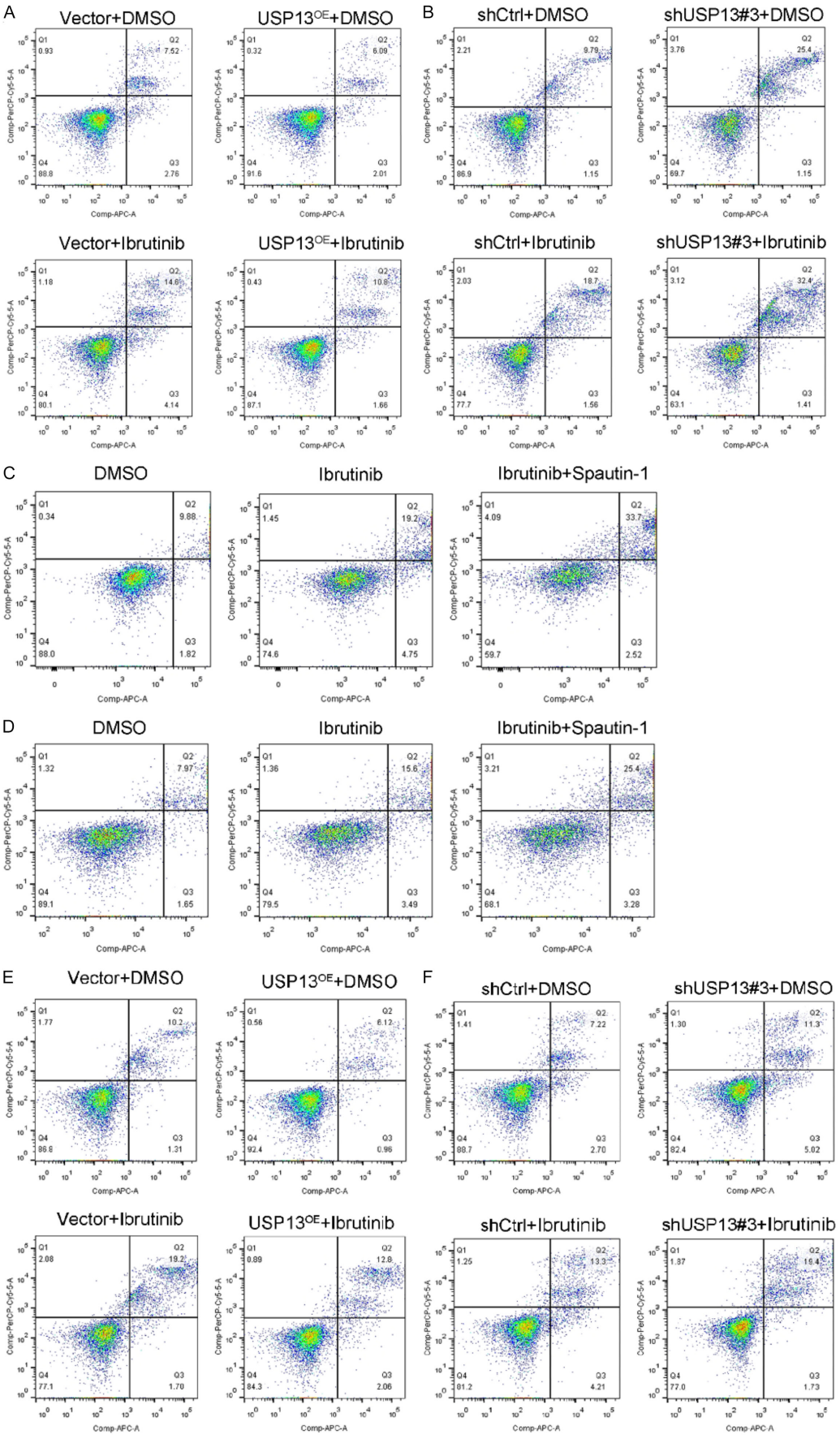
A
Vector+DMSO
USP13OE+DMSO
B
shCtrl+DMSO
shUSP13#3+DMSO
Vector+Ibrutinib
USP13OE+Ibrutinib
shCtrl+Ibrutinib
shUSP13#3+Ibrutinib
C
DMSO
Ibrutinib
Ibrutinib+Spautin-1
D
DMSO
Ibrutinib
Ibrutinib+Spautin-1
E
Vector+DMSO
USP13OE+DMSO
F
shCtrl+DMSO
shUSP13#3+DMSO
Vector+Ibrutinib
USP13OE+Ibrutinib
shCtrl+Ibrutinib
shUSP13#3+Ibrutinib
Comp-PerCP-Cy5-5-A
Comp-APC-A

Supplementary Figure 1. Representative images of apoptosis in WSU-DLCL2 and U2932. A: Apoptosis induced by Ibrutinib in USP13 overexpression (USP13^{OE}) or control (Vector) WSU-DLCL2. B: Apoptosis induced by Ibrutinib in USP13 knockdown (shUSP13#3) or negative control (shCtrl) U2932. C: Apoptosis of U2932 induced by DMSO, Ibrutinib or Ibrutinib and Spautin-1. D: Apoptosis of WSU-DLCL2 induced by DMSO, Ibrutinib or Ibrutinib and Spautin-1. E: Apoptosis induced by Ibrutinib in USP13 overexpression (USP13^{OE}) or control (Vector) U2932. F: Apoptosis induced by Ibrutinib in USP13 knockdown (shUSP13#3) or negative control (shCtrl) WSU-DLCL2.

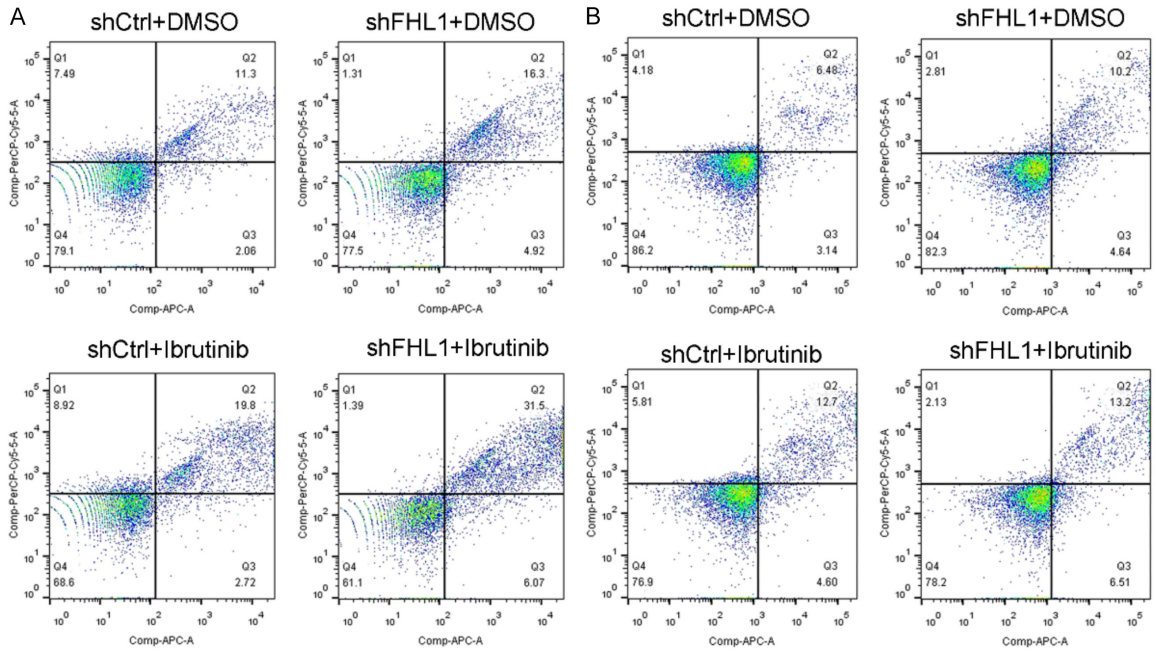

Supplementary Figure 2. Representative images of apoptosis in WSU-DLCL2 and U2932. A: Apoptosis induced by Ibrutinib in FHL1 knockdown (shFHL1) or negative control (shCtrl) U2932. B: Apoptosis induced by Ibrutinib in FHL1 knockdown (shFHL1) or negative control (shCtrl) WSU-DLCL2.

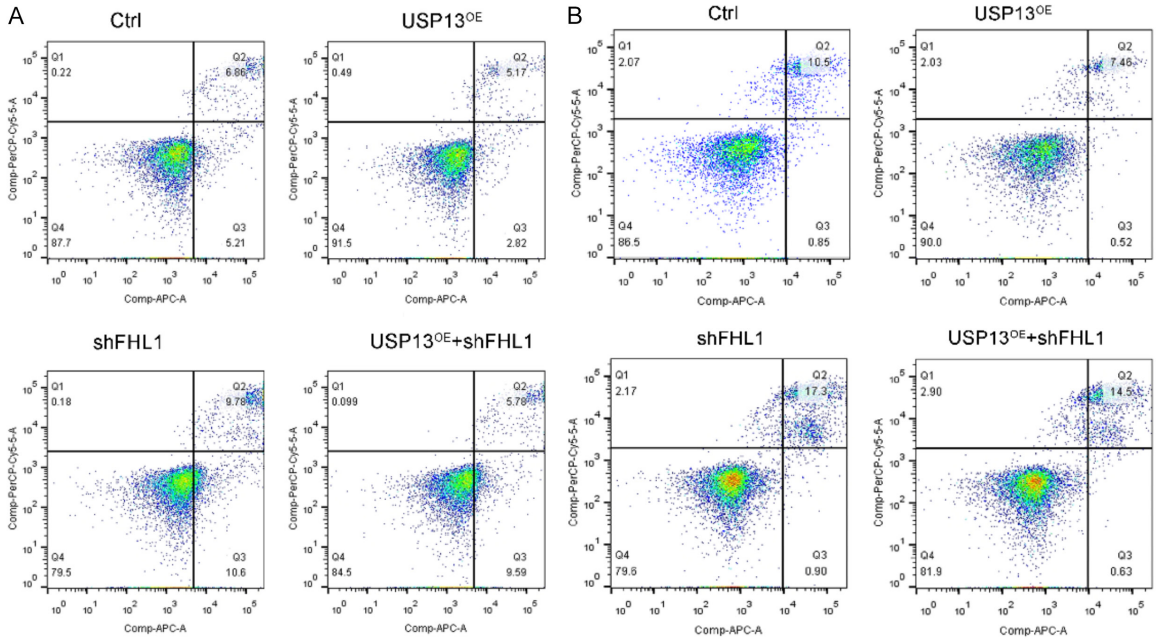

Supplementary Figure 3. Representative images of apoptosis in WSU-DLCL2 and U2932. A: Apoptosis in negative control (Ctrl), USP13 overexpression (USP13^{OE}), FHL1 knockdown (shFHL1) or USP13 overexpression plus FHL1

knockdown (USP13^{OE}+shFHL1) U2932. B: Apoptosis in negative control (Ctrl), USP13 overexpression (USP13^{OE}), FHL1 knockdown (shFHL1) or USP13 overexpression plus FHL1 knockdown (USP13^{OE}+shFHL1) WSU-DLCL2.

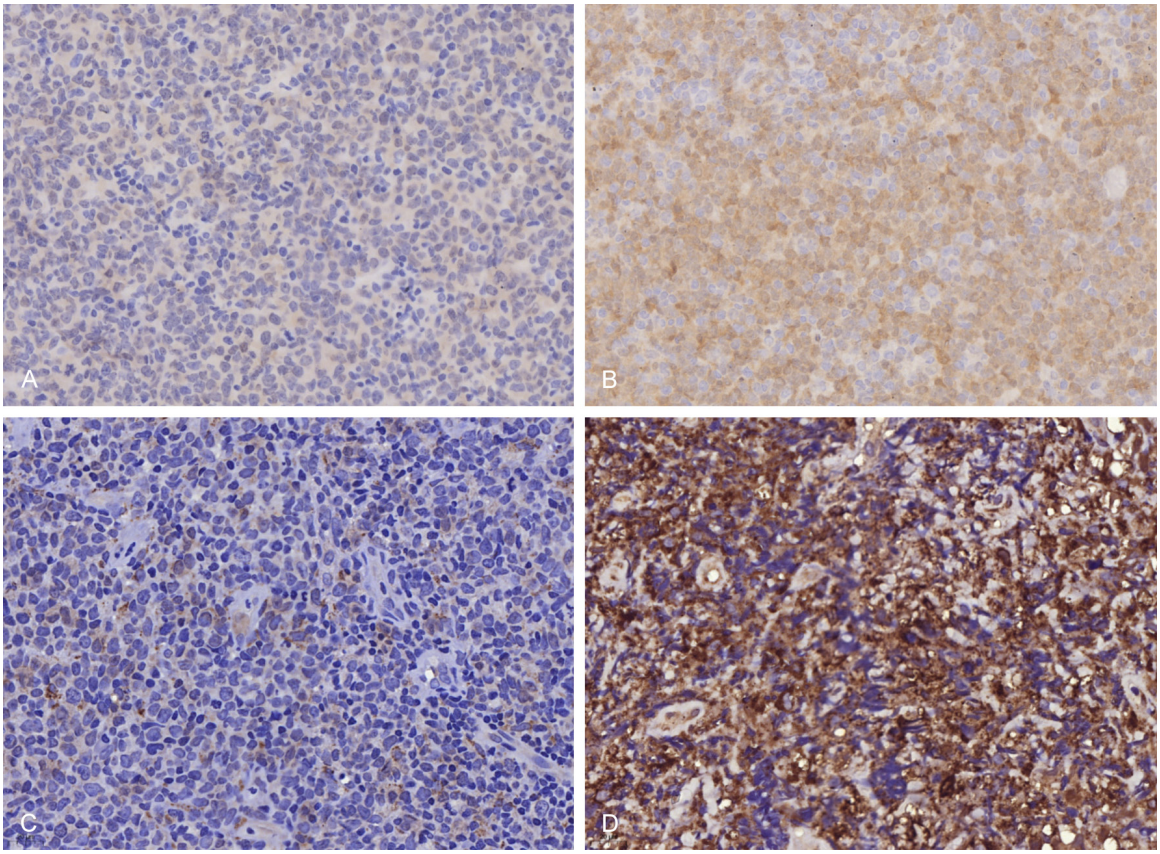

Supplementary Figure 4. Representative images of the immunohistochemistry results of USP13 and FHL1. A: USP13 Low. B: USP13 High. C: FHL1 Low. D: FHL1 High.